

A Transmission Line Matrix Model for Shielding Effects in Stents

Razvan Ciocan ⁽¹⁾, Nathan Ida ⁽²⁾

⁽¹⁾ Clemson University
Physics and Astronomy Department
Clemson University, SC 29634-0978
ciocan@CLEMSON.EDU

⁽²⁾ The University of Akron
Department of Electrical and Computer Engineering
Akron, Ohio 44325-3904
ida@uakron.edu

Abstract

In an attempt to determine the RF shielding artifacts produced by conducting stents during MRI scanning of patients, a Transmission Line Matrix (TLM) model was developed based on the symmetrical condensed node. This approach allows considerable flexibility including freedom from stability issues and the ability to reconstruct digital signals in the time or frequency domain. To validate the results of the model, simplified phantom stents were built, embedded in a gelatinous substance, scanned and the MR data compared directly with the TLM data. The ultimate purpose of the model is enhancement of MR data in stents by compensation of the artifacts with numerically generated data. By subtraction of the shielding artifacts, the MR image can be substantially enhanced. The results obtained from the TLM model compare very well with those obtained with MRI and are within the experimental error expected from MR data. Subtraction of the TLM data from experimental MR data shows significant enhancement in the contrast within the stent.

Keywords: Transmission Line Matrix, contrast enhanced MRA, RF shielding, stent phantoms.

1. Introduction

In routine MR scanning of patients who have received metallic stents, the interior of the stent shows very little contrast due to RF shielding of the stent. Yet it is exactly the interior of the stent that is the main focus of routine scans. It is thus useful to look for means of enhancing the contrast within the volume of the stent. If the shielding effects of the stent can be predicted accurately, these can be subtracted from the MRI image to enhance the contrast in the stent. To that end, a model, based on the Transmission Line Matrix method [1], capable of modeling the intricacies of the stent's structure at the frequencies of interest (64 MHz) has been developed. The model is based on the Transmission Line Matrix (TLM) method that in turn employs a symmetrical condensed node (SCN) [2] as the basic building block. The present development follows the success of the TLM method in other areas [3,4] and its flexibility in modeling both the geometry and the fields in and around the stent. The model has been used initially to demonstrate the capability of the method and the procedure for image enhancement through use of simplified, phantom stents made of aluminum foil and embedded into a gelatinous matrix which simulates body tissue. It is anticipated that a model of this type

can be used in conjunction with scanned data to display enhanced images of the stent and thus aid in evaluation of patients. These developments are described in this paper.

2. The Transmission Line Matrix model

The TLM method is traditionally explained in terms of the equivalence between field quantities and electric quantities (voltages and currents). Discretization is introduced by a set of basis functions that form a Hilbert space. In this space the electromagnetic fields are seen as vectors and the Maxwell operators form matrices. By choosing a basis function set, composed of triangular time functions and pulse spatial functions, the TLM algorithm becomes:

$$\mathbf{v}_t^r = \mathbf{S}\mathbf{v}_t^i, \quad (1)$$

$$\mathbf{v}_{t+1}^i = \mathbf{C}\mathbf{v}_t^r, \quad (2)$$

Here \mathbf{v}_t^r and \mathbf{v}_t^i are two 12-dimensional vectors at the instant t formed by the electric and magnetic fields, \mathbf{E}, \mathbf{B} , at the boundaries of a cell formed by the pulse spatial functions, and \mathbf{S} is a 12-dimensional scattering matrix describing the dynamic evolution of the field vectors. The wave propagation is modeled by the so called connection process, described by matrix \mathbf{C} . In this process, the reflected pulse for a certain node at the instant t becomes the incident pulse for the neighboring nodes at instant $t+1$.

Equations (1) and (2) define the 3D transmission-line matrix (TLM) method, with the following intuitive interpretation. The continuous space is discretized into a network of nodes, each node consisting of 6 interfaces connected by 6 lines, and two ports on each interface, corresponding to 2 polarizations carried on a transmission line pairs. The three index notations used for voltages are related to the position of the ports and the direction of link lines. For example, V_{xpy} , is the voltage pulse on a link line parallel to the x axis, on the positive side, and polarized in the y direction.

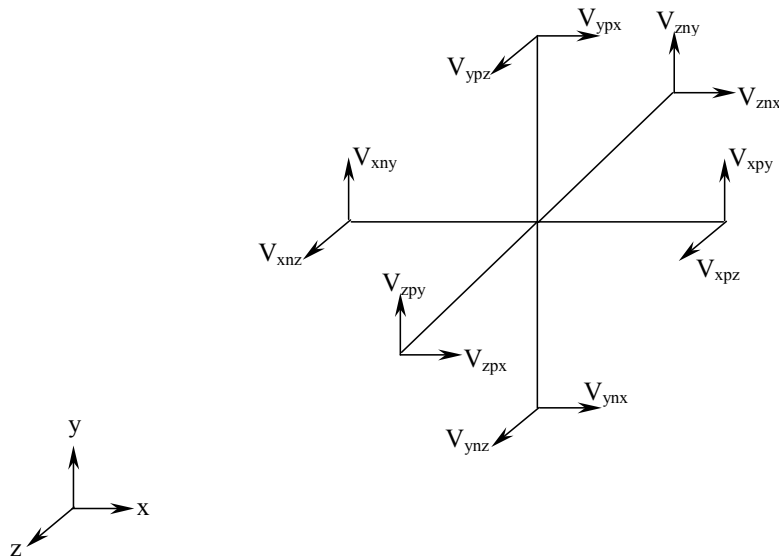


Figure 1 Symmetrical condensed node with the corresponding voltages at ports

In this formulation the field quantities can be written in a more intuitive fashion. For example, the x- components of the electric and magnetic fields are given by:

$$E_x = -\frac{1}{2\Delta x} (V_{ynx}^i + V_{ypx}^i + V_{zpx}^i + V_{zpy}^i) \quad (3)$$

$$H_x = \frac{V_{zny} - V_{ynz} + V_{ypz} - V_{zpy}}{2Z_0\Delta x} \quad (4)$$

where Z_0 is the intrinsic impedance in the medium and Δx is the basic mesh dimension (i.e. the length of the TLM cell). Although not strictly necessary, the cell is usually assumed to be cubic with $\Delta x = \Delta y = \Delta z$.

TLM is a time-domain method, representing a true computer simulation of the wave propagation in the time domain. For a given initial condition (such as a Dirac delta input pulse), all field components in space-time are then determined by equations (1) and (2) without matrix inversion, the numerical stability of which concerns many other numerical methods. The unconditional numerical stability of the TLM method is our rationale for choosing TLM to calculate the RF shielding by stents. Our initial results with stents of simplified geometry demonstrate that this TLM approach is feasible and rather efficient.

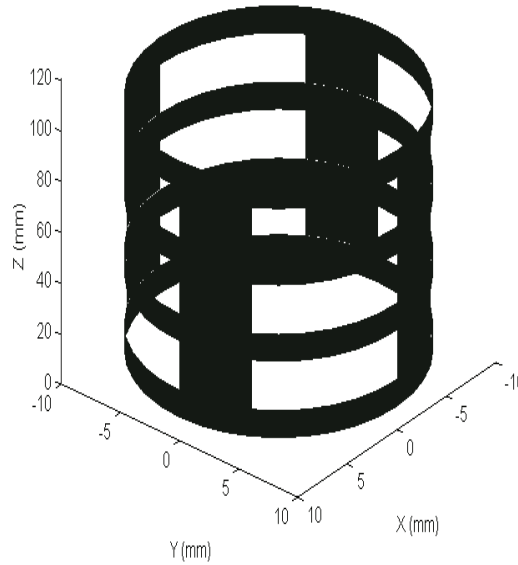


Figure 2. Phantom stent model, 20 mm in diameter, 100 mm long, with 12 symmetric holes, each 20 mm long and encompassing a 60° section.

3. Results

A uniform magnetic field distribution was obtained using a cylindrical field source placed concentrically with the phantom stent. This source has a diameter twice that of the phantom stent model. The phantom stents were then embedded in 1% gadolinium doped agar (gelatin). Imaging was performed on a 1.5T scanner using a head coil and a 3D fast spoiled gradient echo (SPGR) pulse sequence. For measuring susceptibility effects, imaging parameters were: TE (Echo Time) = 1.8ms, TR

(Repetition Time) = 8ms, FOV (Field of View) = 20 mm, acquisition matrix = 256x256x8, slice thickness = 1mm, flip angle = 40°.

A phantom stent used in preliminary experiments is shown in Fig. 2. The phantom was made from 7 μm thick aluminum foil tape. It is a cylinder, 20 mm in diameter and 100 mm in length, with 12 symmetrical holes in it, each hole a rectangle, 20 mm long and spanning a 60° angle.

The MRI scan and the TLM simulation are shown in Fig. 3a and 3b. The results and errors depend on the size of the “holes”. A number of these phantoms were built and tested. The TLM data was then subtracted from the MRI data to remove the shielding effects of the conducting stent. Figure 4 shows this result. The interior of the stent is much brighter indicating that the effects of the stent shielding have been largely removed.

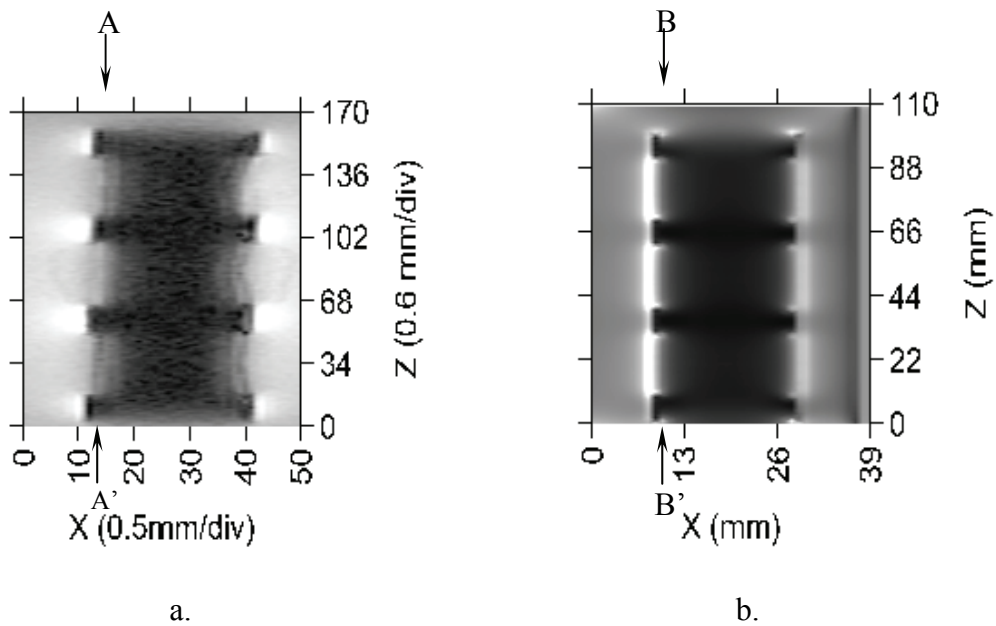


Figure 3. a. MRI image obtained by interpolating the original experimental MRI data. b. TLM image obtained by interpolating the original numerical data.

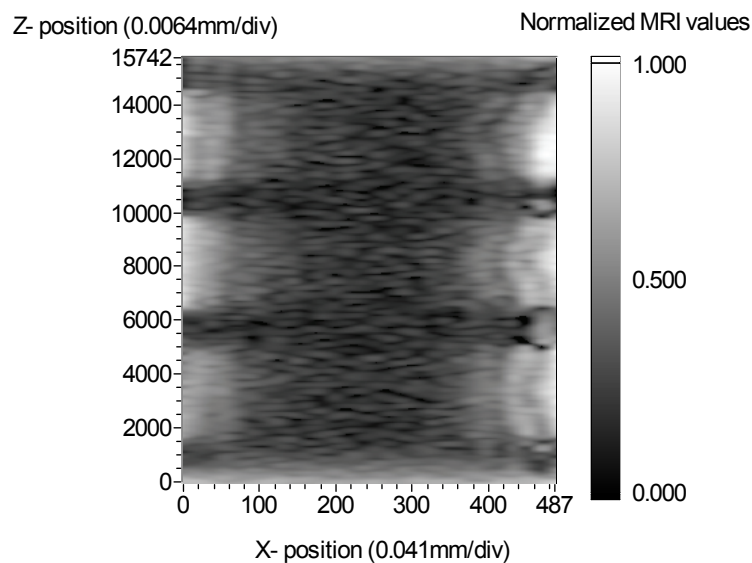


Figure 4. Difference image, obtained by subtracting the TLM image (figure 3b) from MRI image (figure 3a), normalized to 1.

Another way of comparing the data is shown in Figure 5. The line indicated as “real profile” indicates the physical profile of the stent showing the holes. The TLM profile is shown in solid lines while the MRI profile in the dark lines at the bottom of the figure. The correspondence of the MRI data with the physical stent is clear. The MRI profile’s intensity is low hence the need for normalization.

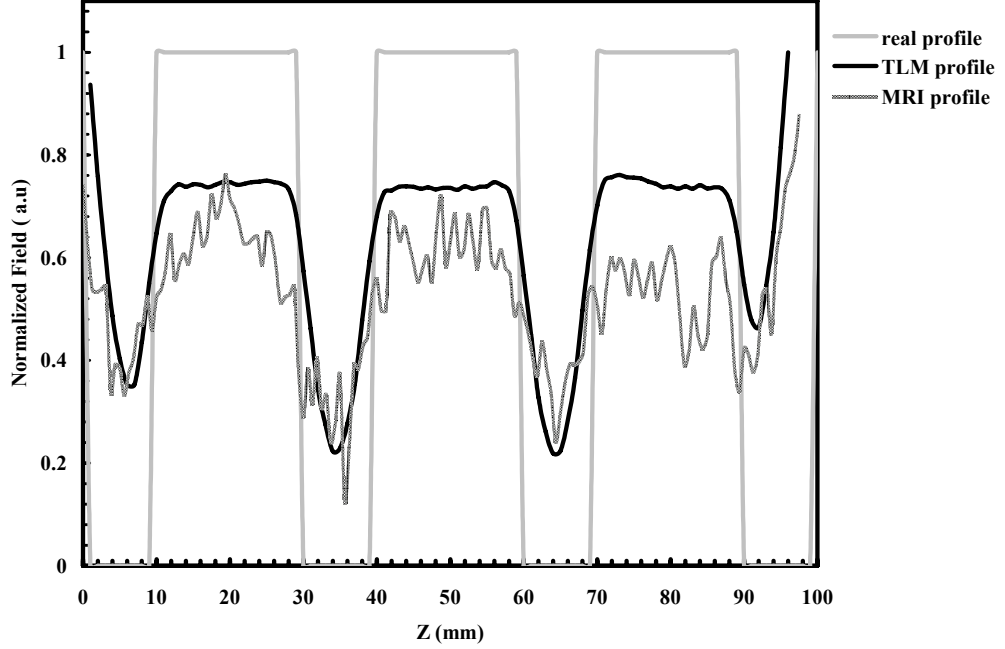


Figure 5. Comparison between two profiles obtained from MRI and TLM images respectively AA' and BB' from figure 3.

The errors associated with the TLM and MRI scans were evaluated from images obtained when the phantom stent was not in place. For this purpose an area of 4 by 4 mm was considered in the same position where the shielding factor will be determined when the phantom stent is in place. The value determined are: $S_{\text{backgroundMRI}} = 220 \pm 21$ (for MRI) and $S_{\text{backgroundTLM}} = 237 \pm 3$ (for TLM). The errors determined in the evaluation of $S_{\text{backgroundMRI}}$ (9.5%) and $S_{\text{backgroundTLM}}$ (1.2%) should be considered in comparison with the results obtained for the factor shielding evaluation from MRI and TLM images. Reduction of the detected signal, $R(x)$, due to shielding was determined for phantoms with different dimensions of holes as follows:

$$R_{MRI} = \sqrt{\frac{S(x)}{S_{\text{backgroundMRI}}}} \quad (5)$$

$$R_{TLM} = \sqrt{\frac{S(x)}{S_{\text{backgroundTLM}}}} \quad (6)$$

The reduction values determined are shown in Table 1. Although the errors between the reduction values for MRI and TLM scans may seem high they are within the limits of measurement errors for the MRI image.

Table 1. Results obtained for the reduction of the detected signal due to shielding

Hole dimension (mm)	TLM	MRI
20 x 10	18.25 %	28.97 %
15 x 10	16.79 %	21.03%
6 x 20	6.56 %	14.25 %
6 x 15	5.0 %	12.6 %

Acknowledgement

The authors gratefully acknowledge Dr. Yi Wang and Cecil Yen from the Department of Radiology, University of Pittsburgh School of Medicine, Pittsburgh, Pennsylvania for providing the data for Figure 2b and for conducting the MRI scans.

References

- [1] Johns, P. B. Beurle, R. L., " Numerical solution of Two-Dimensional Scattering Problems Using a Transmission-Line Matrix," *Proc. IEEE*, vol 118, pp 1203-1209, 1971.
- [2] Johns, P. B., "A symmetrical condensed node for the TLM method," *IEEE Transaction on Microwave Theory and Techniques* vol. MTT_35 No.4 pp. 370-377, 1987.
- [3] Ciocan, R. and N.Ida, "Transmission Line Matrix Model for Detection of Local Changes in Permeability Using a Microwave Technique," *IEEE Transactions on Magnetics*, Vol. 40, No. 2, march 2004, pp.651-654.
- [4] Ciocan R., N. Ida, E. Ciocan and H. Jiang, "Applications of the Transmission Line Matrix Method to Microwave Scanning Microscopy," *ACES Journal*, Vol. 19, No. 1b, March 2004, pp. 94-100.